

Fig. 4. Slowing factor versus width-to-height ratio  $a/b$ . Open circles: experimental values. Solid lines: theoretical values. Dashed lines: slowing factor in the infinitely wide strip case. 1: delay data in [2].

quantity is also equal to the ratio of the propagation velocity to the light velocity in vacuum. As seen from the figure, the propagation velocity is constant and very slow in the lower frequency region. Let this region be defined as the slow mode region. In the figure, the propagation velocity in the slow mode region is from approximately 1/15 to 1/20 of the light velocity, and is essentially smaller than that of TEM propagation through the SiO<sub>2</sub> of the Si layer. While the values of the characteristic impedance and propagation velocity appear to be almost independent of the substrate resistivity in this region, the upper frequency limit of the region clearly depends upon it, and becomes maximum for the 10<sup>-1</sup> Ω·cm sample, extending into the low-gigahertz region. Outside the slow mode region, the characteristic impedance increases with frequency for higher resistivity and decreases for lower resistivity. Further, the attenuation constant in the mid-frequency range increases approximately in proportion to the square of the frequency, and is minimum for the 10<sup>-1</sup> Ω·cm sample. All these features are qualitatively in good agreement with the numerical result [1]. Disagreement in the attenuation constant in the low-frequency region can be explained by the finite resistance of the strip conductor ignored in the theoretical computation, and this explanation has been confirmed quantitatively by measuring the sheet resistivity of the experimental strips.

Further, the slow wave propagation velocity was measured varying the strip width, and the result is plotted in Fig. 4 in terms of the slowing factor defined by  $\lambda_0/\lambda_g$ , versus the width-to-height ratio  $a/b$ . The thickness ratio  $b_1/b_2$  is held nearly constant for all the samples within the range from  $4 \times 10^{-3}$  to  $5 \times 10^{-3}$ . The propagation delay data in [2] are also included in the figure. Solid lines give the theoretical values based on the quasi-static approach using the formula for microstrip fringing fields [3]. Agreement between the theory and the experiment is generally good, both indicating a decrease in the slowing factor due to the fringing effect with a decreasing width-to-height ratio.

In conclusion, the slow wave mode does propagate along the microstrip line on Si-SiO<sub>2</sub> systems, with its upper frequency limit depending on the substrate resistivity. This mode of propagation seems to be of great importance to the current monolithic IC's, judging from the values of resistivity and frequency usually employed.

The physical mechanism of slow wave propagation can be attributed to the large effective dielectric constant due to the strong interfacial polarization (Maxwell-Wagner mechanism [4]), from which there results a slow surface-wave-like propagation. A detailed theoretical and experimental analysis of this type of line, including the slow mode mechanism and the behavior of other fundamental modes, will be presented in a forthcoming paper.

ACKNOWLEDGMENT

The authors wish to thank the technical staffs of the Nippon Electric Co., Ltd., IC Division, for useful discussions and for providing the experimental samples.

HIDEKI HASEGAWA<sup>1</sup>  
 MIEKO FURUKAWA  
 HISAYOSHI YANAI  
 Dep. of Electron. Eng.  
 University of Tokyo  
 Tokyo, Japan

REFERENCES

- [1] H. Guckel, P. A. Brennan, and I. Pačóć, "A parallel-plate waveguide approach to microminiaturized, planar transmission lines for integrated circuits," *IEEE Trans. Microwave Theory Tech.*, vol. MTT-15, Aug. 1967, pp. 468-476.
- [2] I. T. Ho and S. K. Mullick, "Analysis of transmission lines on integrated-circuit chips," *IEEE J. Solid-State Circuits*, vol. SC-2, Dec. 1967, pp. 201-208.
- [3] M. V. Schneider, "Microstrip lines for microwave integrated circuits," *Bell Syst. Tech. J.*, vol. 48, May 1969, pp. 1421-1444.
- [4] A. R. von Hippel, *Dielectrics and Waves*. New York: Wiley, 1954, p. 228.

<sup>1</sup> Presently with Dep. of Elec. Eng., Hokkaido University, Sapporo, Japan.

Computation of Spectra with Unequal Resolution Using the Fast Fourier Transform

**Abstract**—The discrete Fourier transform of a sequence, which can be computed using the fast Fourier transform algorithm, represents samples of the  $z$  transform equally spaced around the unit circle. In this letter, a technique is discussed and illustrated for transforming a sequence to a new sequence whose discrete Fourier transform is equal to samples of the  $z$  transform of the original sequence at unequally spaced angles around the unit circle.

In many applications we are concerned with the problem of computing samples of the  $z$  transform of a sequence on the unit circle. To obtain samples equally spaced around the unit circle, the most efficient procedure is to compute the discrete Fourier transform (DFT) using the fast Fourier transform (FFT) algorithm.<sup>1</sup> If we are interested in obtaining samples equally spaced within a particular region of the unit circle, then one efficient procedure consists of using the chirp  $z$ -transform algorithm.<sup>2</sup> Often we would like to obtain samples that are unequally spaced—corresponding, for example, to a constant  $Q$  spectral analysis of the original sequence. An algorithm for accomplishing this with an efficiency similar to that achievable with the FFT algorithm is not known. One procedure sometimes used is to evaluate the samples explicitly at the desired frequencies. Another procedure used is to add equally spaced frequency samples in bands. A related alternative procedure corresponds to implementing a spectral analysis of the sequence with a recursive or nonrecursive filter bank. This letter is directed toward a procedure that perhaps is slightly more efficient than the alternative just mentioned, and may also have some advantages when considering hardware implementation of a spectral analysis with nonuniform resolution.

The procedure consists of transforming the original sequence to a new sequence having the property that its DFT is equal to samples of the  $z$  transform of the original sequence at unequally spaced angles around the unit

Manuscript received June 11, 1970; revised July 30, 1970. A. Oppenheim and D. Johnson were supported in part by the Joint Services Electronics Programs under Contract DA-28-043-AMC-02536(E) and by the U. S. Air Force Cambridge Research Laboratories, Office of Aerospace Research, under Contract F19628-69-C-0044. K. Steiglitz was supported in part by the U. S. Army Research Office, Durham, N. C., under Contract DAHCO4-69-C-0012.

<sup>1</sup> J. W. Cooley and J. W. Tukey, "An algorithm for the machine calculation of complex Fourier series," *Math. Comput.*, vol. 19, pp. 297-301, April 1965.

<sup>2</sup> L. Rabiner, R. Schafer, and C. Rader, "The chirp  $z$ -transform algorithm and its applications," *Bell Syst. Tech. J.*, vol. 48, pp. 1249-1292, May-June 1969.

circle.<sup>3</sup> Letting  $f(n)$  represent the original sequence, and  $g(k)$  represent the transformed sequence, we consider linear transformations between  $f(n)$  and  $g(k)$  corresponding to expanding  $f(n)$  in terms of a set of linearly independent sequences  $\psi_k(n)$  so that

$$f(n) = \sum_{k=-\infty}^{+\infty} g(k)\psi_k(n). \tag{1}$$

The basic property that we would like this transformation to have is that the  $z$  transform of the sequence  $f(n)$  and the  $z$  transform of the sequence  $g(k)$  are related by a change of variables, so that on the unit circle, if

$$G(e^{j\omega}) = \sum_{k=-\infty}^{+\infty} g(k)e^{-j\omega k}$$

and

$$F(e^{j\Omega}) = \sum_{n=-\infty}^{+\infty} f(n)e^{-j\Omega n}$$

then

$$\omega = \theta(\Omega)$$

so that

$$G(e^{j\theta(\Omega)}) = F(e^{j\Omega}). \tag{2}$$

Consequently, what is required is that the Fourier transform of  $f(n)$  and the Fourier transform of  $g(k)$  be related by a distortion of the frequency axis. It can be shown that the requirement placed on the set of functions  $\psi_k(n)$  such that (2) is satisfied is that

$$\Psi_k(e^{j\Omega}) = e^{-jk\theta(\Omega)} \tag{3}$$

where

$$\Psi_k(e^{j\Omega}) = \sum_{n=-\infty}^{+\infty} \psi_k(n)e^{-j\Omega n}.$$

Therefore, the functions  $\psi_k(n)$  must have an all-pass characteristic, that is, their  $z$  transform on the unit circle must have unity magnitude independent of frequency. With these conditions satisfied, the relationship between the frequency variable  $\omega$  corresponding to the Fourier transform of the new sequence  $g(k)$  and the frequency variable  $\Omega$  corresponding to the Fourier transform of the original sequence  $f(n)$  is that

$$\omega = \theta(\Omega). \tag{4}$$

If we restrict the mapping from  $\Omega$  to  $\omega$  to be such that when  $\Omega$  changes by  $2\pi$  then  $\omega$  changes by  $2\pi$ , and if we require that the  $z$  transform  $\Psi_k(z)$  of the functions  $\psi_k(n)$  be rational functions of  $z$ , then  $\Psi_k(z)$  must be of the form

$$\Psi_k(z) = \left( \frac{z^{-1} - a}{1 - az^{-1}} \right)^k. \tag{5}$$

As required, the magnitude of  $\Psi_k(z)$  for  $z$  on the unit circle is unity, and the phase factor  $\theta(\Omega)$  is given by

$$\omega = \theta(\Omega) = \tan^{-1} \left[ \frac{(1 - a^2) \sin \Omega}{(1 + a^2) \cos \Omega - 2a} \right]. \tag{6}$$

It can be shown that the inverse relation is

$$\Omega = \theta^{-1}(\omega) = \tan^{-1} \left[ \frac{(1 - a^2) \sin \omega}{(1 + a^2) \cos \omega + 2a} \right] \tag{7}$$

which corresponds to replacing  $a$  by  $-a$  in (6). Consequently, (6) specifies the relationship between the new frequency variable  $\omega$  and the original

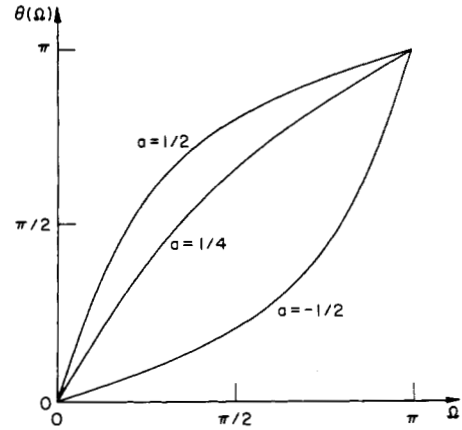


Fig. 1. Distortion of frequency for several values of  $a$ .

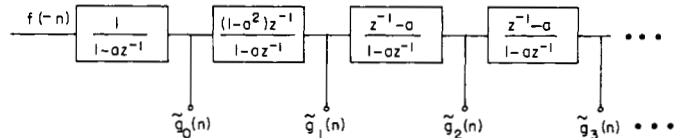


Fig. 2. All-pass network used to implement a distortion of the frequency axis.

frequency variable  $\Omega$ . Since a computation of the DFT of the new sequence  $g(k)$  corresponds to sampling uniformly in  $\omega$ , the frequency samples obtained will correspond to nonuniform sampling in the original frequency variable  $\Omega$ . Fig. 1 shows the function  $\theta(\Omega)$  for several values of the parameter  $a$ .

For the remainder of the discussion, we will assume that  $f(n)$  and  $g(k)$  are both zero for  $n < 0$ . It is straightforward to modify the discussion to incorporate the more general case. For the particular functions  $\psi_k(n)$  defined by (5), it can be shown that

$$\sum_{n=0}^{\infty} n\psi_r(n)\psi_k(n) = k, \quad r = k$$

$$= 0, \quad r \neq k.$$

Consequently, this set of functions  $\psi_k(n)$  is orthogonal with a weighting function of  $n$  and a normalizing constant of  $k$ . From this relation together with (1), the sequence  $g(k)$  is specified by

$$g(k) = \frac{1}{k} \sum_{n=0}^{\infty} n\psi_k(n)f(n), \quad k = 1, 2, \dots \tag{8a}$$

$$g(0) = \sum_{n=0}^{\infty} f(n)a^n. \tag{8b}$$

One implementation of (8) consists of passing the sequence  $f(-n)$  through the linear shift-invariant network shown in Fig. 2. With the outputs in the network of Fig. 2 designated as  $\tilde{g}_k(n)$ , the sequence  $g(k)$  is related to  $\tilde{g}_k(n)$  by

$$g(k) = \tilde{g}_k(0).$$

To obtain the samples of the spectrum of the original sequence on the distorted frequency scale, the DFT of the sequence  $g(k)$  is computed. From the curves in Fig. 1, with the parameter  $a$  real and between 0 and 1, the effect on the spectrum is to sample with higher resolution at low frequencies and lower resolution at higher frequencies. If, instead,  $a$  is negative, between 0 and  $-1$ , then the effect is the reverse, that is, the spectrum is sampled with greater resolution at higher frequencies than at low frequencies. It is also straightforward to implement the network in Fig. 2 with a complex value for  $a$ . This would then result in high spectral resolution at some intermediate frequency.

In general, if the sequence  $f(n)$  is of finite duration, the sequence  $g(k)$  will be of infinite duration. Consequently, in order to compute the DFT

<sup>3</sup> A. Oppenheim and D. Johnson, "Discrete representations of analog signals," M.I.T. Res. Lab. Electron., Cambridge, Mass., Quart. Progr. Rep. 97, pp. 185-190, April 15, 1970.

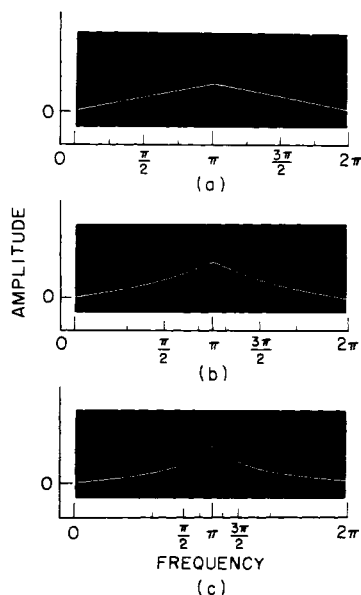


Fig. 3. Example of frequency distortion. (a) Original spectrum. (b) Distorted spectrum with  $a = 1/4$ . (c) Distorted spectrum with  $a = 1/2$ .

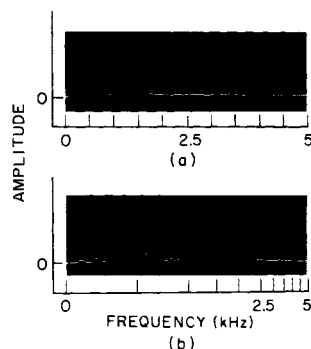


Fig. 4. Example of frequency distortion on a sample of speech. (a) Original spectrum. (b) Distorted spectrum with  $a = 1/2$ .

of  $g(k)$ , an appropriate finite-duration window must be applied. Applying such a window corresponds to “smearing” the spectrum of the sequence before obtaining the spectral samples. The spectral window applied to the transform of  $g(k)$  maintains constant width in  $\omega$  which corresponds to smearing the spectrum of  $f(n)$  with unequal bandwidth. From (6) it follows that for  $a > 0$ , the bandwidth of the spectral window increases with frequency in the same way that the spacing of the spectral samples increases with frequency. This is similar (but not identical) to the situation where a spectral analysis is implemented by implementing a constant  $Q$  filter bank, in which case both the spacing of the spectral samples and the bandwidth of the filter increase with increasing frequency.

Examples of spectral analysis implemented on the basis of this discussion are illustrated in Figs. 3 and 4. Fig. 3(a)–(c) corresponds to the DFT of an original sequence and the transformed sequences for  $a = \frac{1}{4}$  and  $a = \frac{1}{2}$ . Similarly, Fig. 4(a) and (b) corresponds to the DFT of an original and a transformed segment of a speech waveform. In all of these spectra, the transform size was 512 points.

ALAN OPPENHEIM  
 DON JOHNSON  
 Dep. of Elec. Eng. and Res.  
 Lab. of Electron.  
 Mass. Inst. Tech.  
 Cambridge, Mass. 02139  
 KENNETH STEIGLITZ  
 Dep. of Elec. Eng.  
 Princeton University  
 Princeton, N. J. 08540

### Comments on “Nonlinear Resistors that Generate Subharmonics”

**Abstract**—The analysis reported by Erdey is shown to be incorrect.

In the above letter,<sup>1</sup> M. R. A. Erdey discusses the response of the nonlinear resistor, characterized by  $v = 2i^2 - 1$ , to the driving voltage  $v = \cos \omega t$ . He points out that there are four possible solutions,

$$\pm \cos \frac{\omega t}{2}, \quad \pm \left| \cos \frac{\omega t}{2} \right|$$

and attempts to identify the correct solution by considering parasitic lead inductance.

Unfortunately, Erdey does not discuss the behavior of the resulting differential equation, but apparently assumes that the presence of inductance will carry  $i$  through the value  $i = 0$ .

If instead of a small residual inductance we consider a small residual resistance, e.g., radiation resistance, the circuit equation becomes

$$\cos \omega t = 2i^2 - 1 + \epsilon i \tag{1}$$

or

$$i \left( i + \frac{\epsilon}{2} \right) = \cos^2 \frac{\omega t}{2} \geq 0. \tag{2}$$

The range  $-(\epsilon/2) < i < 0$  is forbidden by this inequality. Therefore,  $i$  cannot change sign, and in the limiting case of  $\epsilon \rightarrow 0$ ,

$$i = \pm \left| \cos \frac{\omega t}{2} \right|.$$

This solution has the period  $T = 2\pi/\omega$ , and there are no subharmonics.

CHESTER H. PAGE  
 Nat. Bur. Stand.  
 Washington, D. C. 20234

Manuscript received August 27, 1970.  
<sup>1</sup> M. R. A. Erdey, *Proc. IEEE* (Letters), vol. 58, pp. 1174–1175, July 1970.

### Work Function Difference Between p-type Polycrystalline Silicon and n-type Single-Crystal Silicon

**Abstract**—The work function difference between p-type polycrystalline silicon and n-type single-crystal silicon has been found from flat-band measurements on MNOS capacitors to be +1.55 V when the concentration in the p-type silicon is  $10^{19}$  atoms/cm<sup>3</sup> and the concentration in the n-type silicon is  $10^{15}$  atoms/cm<sup>3</sup>.

It is well known that one way to achieve a low threshold voltage in MOS devices is to use a silicon gate [1], [2] since the threshold voltage is determined in part by the work function difference between the gate and the silicon substrate. For a conventional MOS structure with aluminum-oxide-silicon, the work function differences from aluminum to silicon are from  $-0.12$  to  $-0.38$  V for n-type silicon and  $-1.08$  to  $-0.82$  V for p-type silicon depending on the impurity concentration of the silicon [3]. It is the purpose of this investigation to determine the work function difference between p-type polycrystalline silicon and an n-type silicon substrate.

One way to derive the work function difference is to determine the flat-band voltage  $V_{FB}$  from the capacitance-voltage characteristics of MOS structures. The flat-band voltage is defined as the voltage applied to the gate to counterbalance the work function difference between the gate and the substrate, and the sheet charge associated with the silicon dioxide-silicon interface [4]: